

INTERNATIONAL JOURNAL OF CHEMICAL REACTOR ENGINEERING

Volume 5

2007

Article A57

Selective Photocatalytic Oxidation of 4-Methoxybenzyl Alcohol to p-Anisaldehyde in Organic-Free Water in a Continuous Annular Fixed Bed Reactor

Vittorio Loddo*

Sedat Yurdakal†

Giovanni Palmisano‡

Gustavo Eduardo Imoberdorf**

Horacio Antonio Irazoqui††

Orlando M Alfano‡‡

Vincenzo Augugliaro§

Hüseyin Berber¶

Leonardo Palmisano||

*Università degli Studi di Palermo, loddo@dicpm.unipa.it

†Anadolu Üniversitesi, sedatyurdakal@yahoo.com

‡Università degli Studi di Palermo, gpalmisano@dicpm.unipa.it

**Universidad Nacional del Litoral CONICET, imoberdorf@intec.unl.edu.ar

††Universidad Nacional del Litoral CONICET, irazoqui@intec.unl.edu.ar

‡‡Universidad Nacional del Litoral CONICET, alfano@intec.unl.edu.ar

§Università degli Studi di Palermo, augugliaro@dicpm.unipa.it

¶Anadolu Üniversitesi, hberber@anadolu.edu.tr

||Università degli Studi di Palermo, palmisano@dicpm.unipa.it

ISSN 1542-6580

Copyright ©2007 The Berkeley Electronic Press. All rights reserved.

Selective Photocatalytic Oxidation of 4-Methoxybenzyl Alcohol to p-Anisaldehyde in Organic-Free Water in a Continuous Annular Fixed Bed Reactor

Vittorio Loddo, Sedat Yurdakal, Giovanni Palmisano, Gustavo Eduardo Imoberdorf, Horacio Antonio Irazoqui, Orlando M Alfano, Vincenzo Augugliaro, Hüseyin Berber, and Leonardo Palmisano

Abstract

Photocatalytic oxidation of 4-methoxybenzyl alcohol to p-anisaldehyde was performed in water organic-free solutions by using a fixed bed continuous photoreactor containing Pyrex beads on which a TiO₂ home prepared photocatalyst was supported. The influence of liquid flow rate, inlet alcohol concentration and catalyst amount on the photoprocess was studied. The highest selectivity to p-anisaldehyde was about 47% being CO₂, the other main oxidation product; traces of 4-methoxybenzoic acid were also detected. The radiation field inside the photoreactor has been modelled by applying the Monte Carlo method thus allowing the determination of the local volumetric rate of photon absorption (LVRPA). It was found that the radiation intensity profile sharply decreases inside the bed so that an important aliquot of the bed is not active for the photoreaction occurrence. This finding indicates that the reactivity results, obtained by measuring the concentration values of reagents and products at the exit of photoreactor, can not be used jointly with the radiation modelling ones for determining the dependence of reaction kinetics on light intensity. The Langmuir-Hinshelwood approach has been satisfactorily applied for modelling the photoreactivity results and the values of all the model parameters have been determined.

KEYWORDS: p-anisaldehyde production, photocatalysis, selective oxidation, titanium dioxide, continuous photoreactor, radiation field modelling

1. INTRODUCTION

Heterogeneous photocatalysis is an advanced oxidation process which has been developed in these last years and involves the photoactivation of semiconductor catalysts. This method allows to oxidise almost all organic and inorganic compounds at room temperature and pressure up to negligible concentration levels and therefore photocatalysis represents a promising alternative technology for the degradation of environmental pollutants present in water or air (Ollis and Al-Ekabi, 1993) and for the inactivation of microorganisms in water (Coronado et al., 2005).

The basic principles of heterogeneous photocatalysis are well established (Schiavello, 1985; Serpone and Pelizzetti, 1989; Schiavello, 1997). When radiations with suitable energy (i.e. equal or higher than the band gap) are absorbed by the semiconductor photocatalyst, electrons, e^- , are promoted to the conduction band leaving holes, h^+ , behind. The photogenerated electron-hole pairs can: (i) recombine, (ii) be trapped in surface states, or (iii) induce redox reactions with species adsorbed onto the catalyst surface. As the first two steps represent a waste of absorbed photons, many efforts are devoted to improve the efficiency of heterogeneous photocatalytic processes (de Lasa et al., 2005). It is worth noting that while a thermal catalyst is always active, a photocatalyst gets active only under irradiation.

Various semiconductor materials (e.g. TiO_2 , ZnO, Fe_2O_3 , CdS, ZnS, etc.) have been tested as oxidation photocatalysts, but it is generally accepted (Fujishima et al., 1999; Fujishima et al., 2000) that TiO_2 anatase is the most reliable material due to its low cost, high photostability and activity; aqueous suspensions of this semiconductor can be activated by radiation with wavelength lower than 380 nm so that TiO_2 can utilize near UV-light and also a small aliquot of solar radiation.

Since very few species are refractory to photocatalytic oxidation, this technology is considered greatly unselective (Hoffmann et al., 1995). Photocatalysis has been however successfully used as a synthetic route for various reactions, as for instance selective cyclization of amino acids (Ohtani et al., 2003), photooxidation of cyclohexane to cyclohexanol and cyclohexanone (Sahle-Demessie et al., 1999; Almquist and Biswas, 2001), selective conversion of adamantane (Cermenati et al., 2003) and sunlight-induced reactions of some heterocyclic bases with ethers (Caronna et al., 2005). Selective oxidation of primary alcohols to aldehydes and ketones has been carried out either in gas phase (Pillai and Sahle-Demessie, 2002) or in liquid phase using acetonitrile as solvent (Mohamed et al., 2002; Farhadi et al., 2005), achieving in some cases high yields.

Recently the feasibility of alcohol partial oxidation by photocatalysis in organic-free water has been reported (Palmisano et al., 2007a): 4-methoxybenzaldehyde (p-anisaldehyde, PAA, a compound used for confectioneries and beverages) was produced from photocatalytic selective oxidation of 4-methoxybenzyl alcohol, MBA. For the photocatalytic process a batch reactor containing aqueous suspensions of commercial and home-prepared TiO_2 (Addamo et al., 2005a) was used; the results indicated that the disappearance of MBA was due to two different reaction pathways occurring in parallel since the start of irradiation, i.e. the partial oxidation to PAA and the total oxidation to CO_2 . The home prepared catalysts, obtained under mild conditions, showed to be much more selective than TiO_2 Merck and TiO_2 Degussa P25 (one of the best photocatalysts generally used for degradation purposes) being the highest selectivity to PAA of ca. 41% for conversion of 65%. This reaction can be considered a simple case of that new branch of chemistry aiming to perform selective conversions of organics solubilised or suspended in water (Narayan et al., 2005; Li and Chen, 2006).

In the industrial practice substituted benzaldehydes are synthesized from the corresponding substituted toluenes in liquid phase in the presence of Co, Ce and Mn salts in acidic medium, through routes that are not atom-efficient. The efficiencies of these processes are not high and high polluting wastes are also produced, causing environmental contamination. In order to overcome these drawbacks this reaction has been carried out in vapour phase by using a series of $V_2O_5/Al_2O_3-TiO_2$ catalysts (Reddy et al., 2006).

In the present investigation the photocatalytic selective oxidation of MBA dissolved in organic-free water was performed in a fixed bed continuous photoreactor by using the home prepared TiO_2 with the best performance for MBA partial oxidation to PAA (Palmisano et al., 2007a); this catalyst was supported on Pyrex glass beads. The aim of the investigation was that of modelling the kinetics of the photoprocess with emphasis on determining its dependence on the radiation field inside the bed. On this ground the influence of liquid flow rate, inlet alcohol

concentration and catalyst amount on the photoreactivity was studied; moreover the values of the Local Volumetric Rate of Photon Absorption (LVRPA) were obtained by using the Monte Carlo approach. It is important to outline that no attempt has been carried out for optimizing the process of aldehyde production and, as a consequence, the operative conditions chosen in this work were those suitable for the kinetic modelling.

2. EXPERIMENTAL

All the photoreactivity experiments were carried out in a continuous annular Pyrex made photoreactor (outer diameter of inner tube, 36 mm; annulus gap, 10.5 mm). A 125 W medium pressure Hg lamp (Helios Italquartz, Italy) was axially positioned inside the reactor; it was cooled by water circulating through a Pyrex thimble. The radiation energy impinging on the reacting volume had an average value of $10 \text{ mW}\cdot\text{cm}^{-2}$. It was measured by using a radiometer UVX Digital, at $\lambda = 360 \text{ nm}$. The inner part of the annulus contained a fixed bed of Pyrex beads (diameter, 2 mm; bed height, 150 mm) covered by a thin layer of home prepared TiO_2 . Figure 1 shows the scheme of the photoreactor. A reservoir of 10 L was used to feed the photoreactor through a peristaltic pump which allowed to vary the liquid flow rate in the $0.1\text{-}1.62 \text{ cm}^3\cdot\text{s}^{-1}$ range.

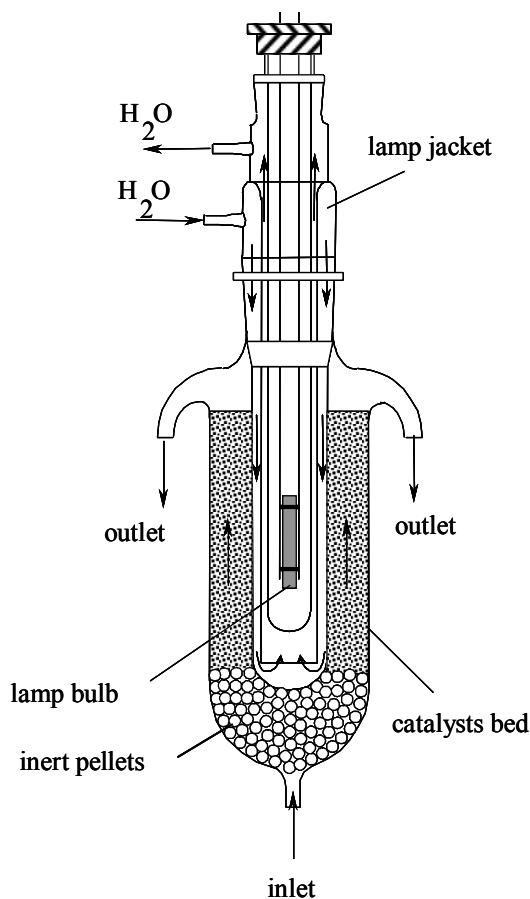


Figure 1. Scheme of photoreactor.

reached steady state conditions in ca. 10 minutes. The run was stopped when three consecutive sample analyses gave the same result, about 40-60 minutes from the starting of irradiation. The inlet substrate concentration of the solution fed to the photoreactor was in the $0.125\text{-}5 \text{ mM}$ range. The pH of the solution was the natural one, i.e. ca. 7. A photoreactivity run was carried out by feeding the reactor with an aqueous solution of PAA (1 mM at pH 7) in order to check the reactivity of this molecule in the used photocatalytic system.

The following procedure was used to prepare the precursor of catalysts (Addamo et al., 2005a). Titanium tetrachloride (Fluka 98%) was used as starting material without any further purification. TiCl_4 was slowly added to distilled water (volume ratios: 1:10) at room temperature. The hydrolysis reaction was highly exothermic and produced high quantities of HCl fumes. After ca. 10 h of continuous stirring, a resulting clear solution was obtained. The Pyrex beads were added to the sol and remained inside it for 30 minutes. After that they were filtered in order to eliminate the supernatant and were placed in a Pyrex tube (maintained at a temperature of 423 K) having a porous frit at the bottom through which a flow of nitrogen was fed for 1.5 h until the TiCl_4 was completely hydrolysed to $\text{Ti}(\text{OH})_4$. A thermal treatment at 673 K for three hours in air was then performed and a thin layer of TiO_2 in anatase phase was obtained, as confirmed by XRD analysis. The procedure was repeated in order to support different layers on the beads (10 or 20 layers). The used supported catalysts are hereafter indicated as HP10 and HP20 in which the figures refer to the number of layers. The total amount of catalyst present in the fixed bed was ca. 3.2 g and 6.0 g for HP10 and HP20, respectively. The estimated thickness of the film was ca. $3.6 \mu\text{m}$ for HP10 and $6.8 \mu\text{m}$ for HP20.

The experimental runs were carried out in the following way. Before starting the feeding of photoreactor the reservoir solution was saturated with oxygen by bubbling pure oxygen for 2 h. The oxygenated solution was fed to the photoreactor until steady state conditions in the dark were reached (i.e. when the outlet MBA concentration was constant), then the lamp was switched on and samples were withdrawn at fixed intervals of time. The photoreactor

The quantitative determination and identification of the species present in the outlet solution was performed by means of a HPLC Beckman Coulter (System Gold 126 Solvent Module and 168 Diode Array Detector), equipped with a Luna 5 μ Phenyl-Hexyl column (250 mm long \times 2 mm i.d.), using Sigma-Aldrich standards. The retention times and UV-spectra of the compounds were compared with an authentic sample. The eluent consisted of: 17.5% acetonitrile, 17.5% methanol, 65% KH₂PO₄ 40 mM aqueous solution. Retention times were 8.7 min for MBA and 17.2 min for PAA and concentrations were calculated at $\lambda = 225$ nm, by using a multi-point calibration curve. All the used chemicals were purchased from Sigma-Aldrich with a purity >99.0%.

XRD patterns of the powders were recorded by a Philips diffractometer using the Cu K α radiation and a 2 θ scan rate of 1.2° min⁻¹.

Total organic carbon (TOC) analyses were carried out by using a 5000A Shimadzu TOC analyser; for each sample six analyses were performed; the mean value was calculated after rejecting the highest and the lowest ones. These analyses aimed to determine the amount of organic carbon mineralized to CO₂.

3. RADIATION MODEL DEVELOPMENTS

In photocatalytic reactions, the photons absorbed by the photocatalyst may be thought as if they collectively were a reactant species. Therefore, the spatial distribution of their absorption rate is an important issue in order to interpret experimental results, to develop kinetic models, and to optimize or scale-up a photocatalytic reactor. The Monte Carlo approach can be employed to obtain the values of the Local Volumetric Rate of Photon Absorption (LVRPA or $e^{a,v}$).

In general terms, the Monte Carlo method applied to the radiation field resolution consists of tracking the trajectory of a great number of photons. In doing that, the basic laws of geometric optics are applied (such as Snell refraction law and Fresnel reflectivity equation), as well as the ray tracing technique. The LVRPA can be constructed out of the series of events that is likely to undergo each of the photons that take part in the simulated experiment. The Monte Carlo method has been successfully employed in the analysis and modelling of photocatalytic reactors (Spadoni et al., 1978; Pasquali et al., 1996; Changrani and Raupp, 1999 and 2000; Yang et al., 2005; Alexiadis, 2006; Imoberdorf et al., 2007).

3.1. Monte Carlo method applied to the fixed bed reactor

In this work, the Monte Carlo method has been applied to obtain the LVRPA at each point in the fixed bed reactor. A similar methodology was applied elsewhere (Imoberdorf et al., 2007). Figure 2 represents the effects taken into account in the current model. Photons may be emitted from every point in the volume of the UV-lamp placed at the centre of the annular reactor (event 1). The emitted photons are assumed to travel along rectilinear trajectories until the internal wall of the reactor is reached (event 2). At this point, photons will change their direction according to the Snell law each time they enter a medium with a different refractive index (event 3). Once in the fluid phase, photons may travel without changing their direction unless they reach a sphere (or eventually one of the reactor walls). If so, they may be reflected back into the fluid phase (event 4); absorbed in the TiO₂ film (event 5); or refracted if they enter the sphere core (event 6). The non-absorbed photons (i.e., those undergoing events 4 or 6, only) continue their rectilinear trajectory until they reach another interface. The photons refracted into a bead core will follow a linear trajectory until they reach the sphere surface from the inside. At this point, the photons may again be reflected back to the solid phase (event 7); absorbed on the TiO₂ film (event 8); or refracted into the fluid phase (event 9). This complex sequence of events will continue until photons are absorbed or leave the reactor. From the photocatalytic point of view, every locally absorbed photon contributes to the LVRPA, and therefore, is responsible for the TiO₂ photo-activation.

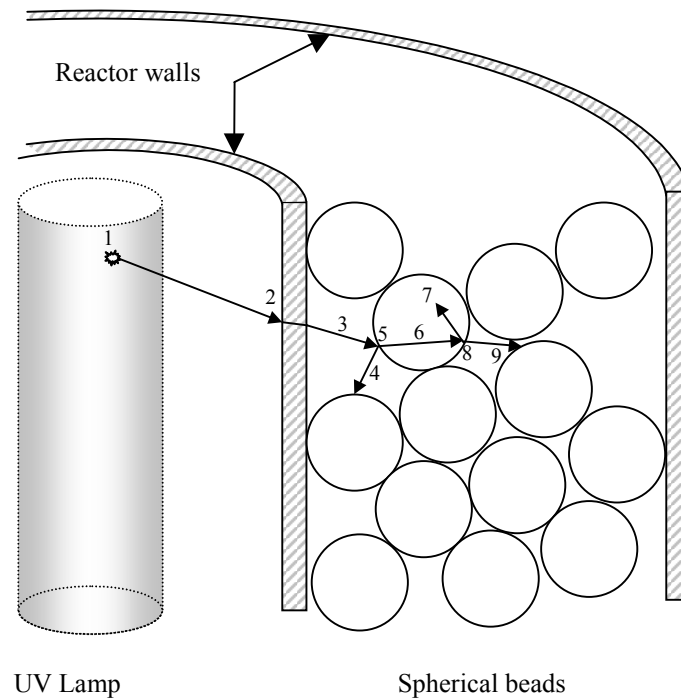


Figure 2. Schematic representation of the photon events taking place in the photocatalytic reactor.

3.2. Assumptions

The model, built for the annular bed made of 2 mm diameter spherical borosilicate glass bead, relies on the followings assumptions: (i) the attenuation of the UV radiation in the borosilicate glass is negligible when compared to the UV absorption in the TiO_2 films; (ii) the TiO_2 films are thick enough to absorb completely the UV radiation (iii) border effects on the sphere spatial distribution in the bed are negligible; (iv) UV photons are emitted by a 3-D Source with Isotropic Volumetric Emission Model (Cassano et al., 1995); (v) photons in the aqueous phase follow straight trajectories until they intercept a sphere surface or a reactor wall; (vi) the mean free path travelled by a given photon in the fluid phase until it collides with a sphere surface is estimated by using the random walk model, the void fraction of the bed, and the radius of the spheres; (vii) the local, angle-dependent reflectivity, at both sides of a sphere surface is calculated by using Fresnel equation; and (viii) the propagation direction of a bundle of photons that have been refracted at the interface between two media with different refraction index is calculated using Snell refraction law.

3.3. Algorithm description

Figure 3 shows a flowchart of the algorithm employed to numerically solve the Monte Carlo model. Firstly, the geometrical dimensions and the optical properties of the reactor and the spherical beads are defined (initiation step). Then, by using five random numbers, it is possible to define both an admissible photon emission point and an admissible photon propagation direction. In this step, the 3-D Source with Isotropic Volumetric Emission Model was applied.

numbers, it is defined whether the photon is reflected, refracted or absorbed by the TiO_2 film covering the sphere. If the photon is absorbed, the location of the absorption point is stored. If the photon is reflected on the bead surface, a new propagation direction is defined by using the specular reflection law, and it is assumed that the photon continues travelling in the aqueous phase. If the photon is refracted, the propagation direction of the photon towards the sphere interior is computed according to Snell law. In this case, the photon will travel inside the sphere without being absorbed because of the high transmittance of borosilicate glass in the range of radiation wavelength considered. Under such situation, the photon will hit the sphere surface ahead of it from the inside. Again, at the collision point the photon can be reflected (undergoing multiple internal reflections); refracted (leaving the sphere to enter the aqueous phase); or can be absorbed by the TiO_2 film. If the photon is absorbed, the location of the absorption point is stored, and a new photon is emitted from the source. This process is repeated for every photon considered. Typically, 10^6 to 10^7 of photons are necessary to obtain accurate results. Once all the photons are tracked, the information about the location of absorption points of each photon is processed in order to obtain the $e^{a,v}$ spatial distribution in the photocatalytic bed.

4. RESULTS

4.1. Photoreactivity

No oxidation of MBA was observed in runs performed in the absence of oxygen and/or light. The contemporary presence of photocatalyst and light determined the MBA oxidation, CO_2 and PAA being the main degradation products detected in the liquid phase. Assuming that no volatile organic compound was formed or its amount was negligible, the decrease of TOC concentration may be ascribed only to CO_2 production. It is worth noting that the values of the mineralized carbon concentration were obtained dividing by 8 the measured TOC values in order to be comparable with the concentrations of the oxidised compound that contains 8 carbon atoms. For each run the mass balance on carbon contained in the outlet stream was verified by adding the MBA and PAA concentrations to that of produced CO_2 and it was always accomplished for more than 99%. Very small amounts of 4-methoxybenzoic acid were also detected. This compound derives from PAA partial oxidation; in fact 4-methoxybenzoic acid and CO_2 were the only products detected in a run carried out with a PAA solution feeding the photoreactor.

Preliminary runs were carried out in order to determine the influence of the liquid flow rate on the MBA oxidation rate, $(-r)$, calculated with the following relation:

$$(-r) = Q(C_{\text{MBA,I}} - C_{\text{MBA,O}}) \quad (1)$$

in which Q is the volumetric liquid flow rate and $C_{\text{MBA,I}}$ and $C_{\text{MBA,O}}$ the molar concentrations of MBA at the inlet and outlet of the photoreactor, respectively. Figure 4 reports the results obtained by experiments carried out with HP10 and HP20 photocatalysts. It may be noted that the same reaction rates are obtained with the two catalysts; moreover for flow rates higher than $0.7 \text{ cm}^3 \cdot \text{s}^{-1}$ the liquid-solid mass transfer resistance plays a negligible role on the photoprocess kinetics. On the basis of this finding all the photoreactivity results have been carried out at a constant flow rate of $0.85 \text{ cm}^3 \cdot \text{s}^{-1}$.

Figure 5 reports the conversion and selectivity for the same experimental runs showed in Figure 4; the conversion, x , and the selectivity, s , are defined as:

$$x \equiv \frac{C_{\text{MBA,I}} - C_{\text{MBA,O}}}{C_{\text{MBA,I}}} \quad (2a)$$

$$s \equiv \frac{C_{\text{PAA,O}}}{C_{\text{MBA,I}} - C_{\text{MBA,O}}} \quad (2b)$$

The data of Figure 5 together with the reaction rate ones indicate that the performance of the two catalysts is independent of the TiO_2 thickness. It can be noticed that in the region in which the external resistances to mass transport play a role, the MBA conversion decreases by increasing the flow rate while the selectivity of the partial oxidation shows an opposite trend. For a differential reactor in diffusional regime the relationship between x and Q can be written by using eqns. 1 and 2a as:

$$x = \frac{(-r)}{Q C_{\text{MBA,I}}} \cong \frac{k_L A_T C_{\text{MBA,I}}}{Q C_{\text{MBA,I}}} = \frac{k_L}{Q} A_T \quad (3)$$

in which A_T is the total transport area of beads. The mass transfer liquid phase coefficient, k_L , depends on $Q^{0.5}$ (Bird et al., 1960) so that the conversion is inversely proportional to Q provided that external mass transfer resistance plays a role. As to concern the increase of selectivity in this region, it may be justified by considering that the PAA concentration values inside the porous photocatalyst are higher at lower flow rates thus favouring the PAA subsequent partial or total oxidation.

Figure 6 shows the results obtained by experimental runs at different inlet MBA concentrations. In this figure the ordinate represents the MBA oxidation rate and the abscissa the arithmetical mean value between the inlet and the outlet MBA concentration. Figure 7 reports the conversions and selectivity for the same experimental runs showed in Figure 6. An improved selectivity towards PAA results with an increase in MBA concentration.

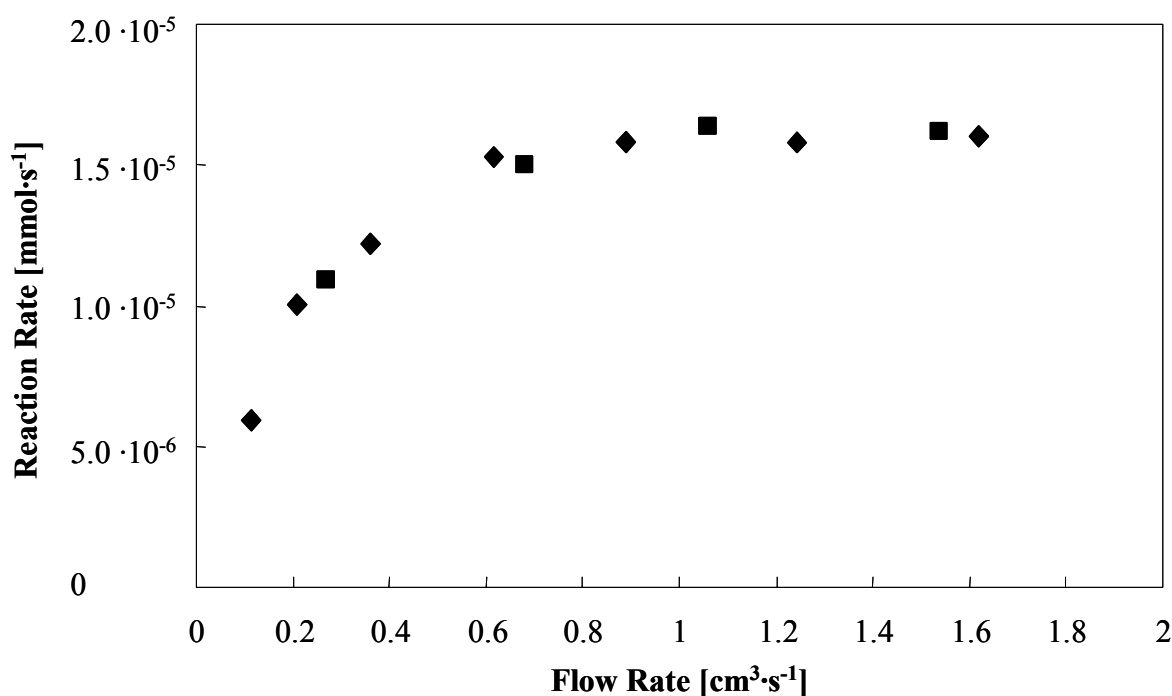


Figure 4. Influence of liquid flow rate on the MBA oxidation rate for experiments carried out with HP10 (♦) and HP20 (■). Inlet MBA concentration: 0.5 mM.

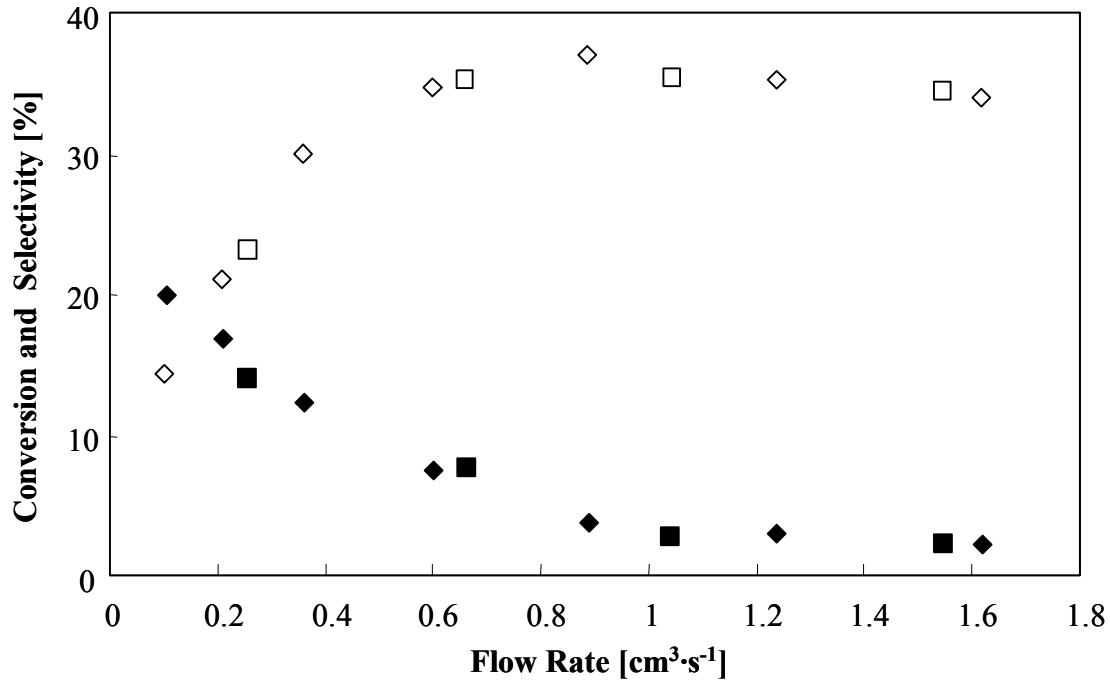


Figure 5. Influence of liquid flow rate on the MBA conversion (full symbols) and selectivity (empty symbols) to PAA for experiments carried out with HP10 (◆, ◇) and HP20 (■, □). Inlet MBA concentration: 0.5 mM.

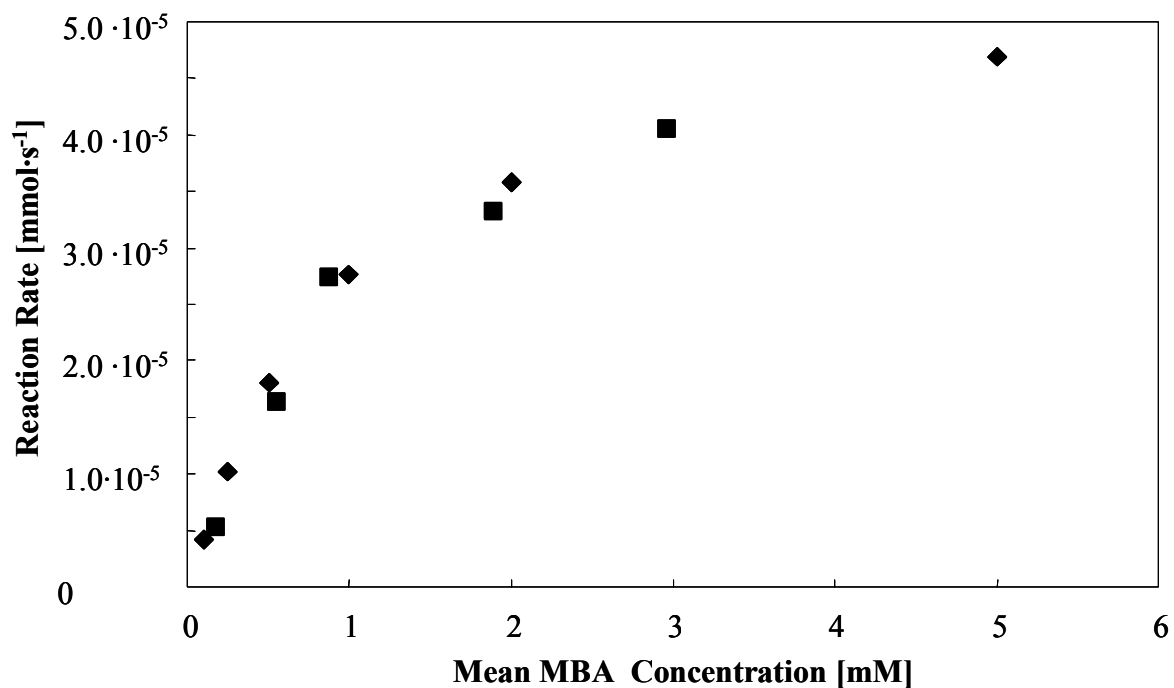


Figure 6. Influence of the mean concentration on the MBA oxidation rate for experiments carried out with HP10 (◆) and HP20 (■). Flow rate: 0.85 cm³·s⁻¹.

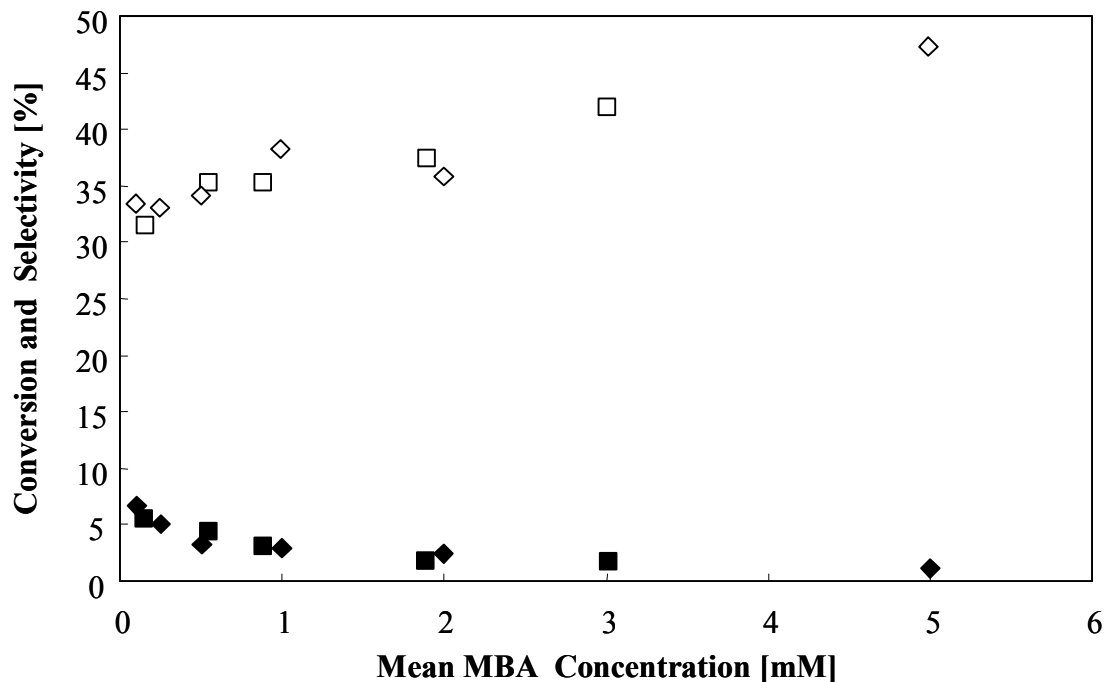


Figure 7. Influence of the mean concentration on the MBA conversion (full symbols) and selectivity (empty symbols) to PAA for experiments carried out with HP10 (◆,◇) and HP20 (■,□). Flow rate: $0.85 \text{ cm}^3 \cdot \text{s}^{-1}$.

4.2. Radiation Modelling Results

Figure 8 shows the values of LVRPA predicted by using the Monte Carlo model as a function of the reactor radius. The sharp slope of this curve implies that the radiation is strongly attenuated for the TiO_2 -coated beads. According to these model results, the sphere layers closer to the inner wall of the annular reactor are the only ones receiving UV-radiation. Most of the spheres remain in dark zones of the photocatalytic bed. Under such conditions, most of the volume of the reactor is not contributing to the photocatalytic reaction.

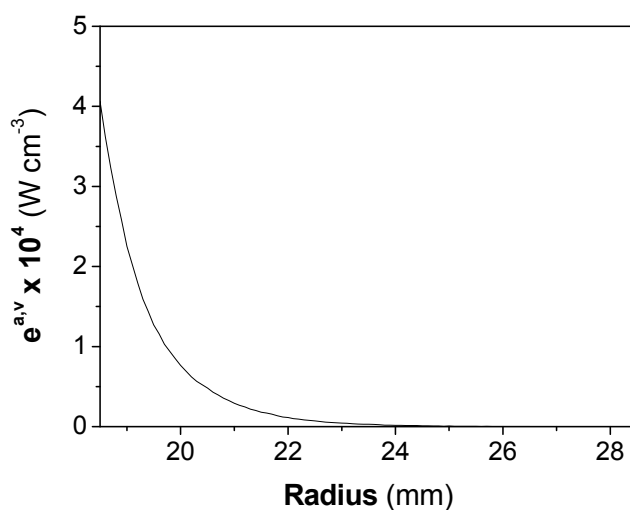


Figure 8. Modelled values of LVRPA against the reactor radius for HP10 and HP20 photocatalysts.

5. DISCUSSION

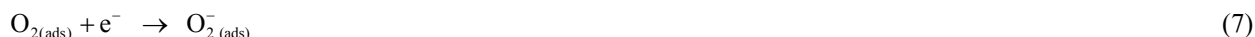
The main feature of heterogeneous photocatalysis is that it involves the photoactivation of the semiconductor catalyst. In fact under irradiation with light of suitable energy the semiconductor oxide is photo-excited producing electron-hole pairs:



The separated pairs can induce redox transformations with species adsorbed onto the catalytic surface according to thermodynamic constraints. It is generally assumed that surface hydroxyl groups act as hole traps producing HO[•] radicals:



Adsorbed oxygen acts as electron trap according to the following equations:



In order that reaction events may occur, it is necessary that photons are absorbed by the photocatalyst as shown by reaction 4. The results obtained by the radiation modelling indicate that an important aliquot of the fixed bed (about one half) is not reached by radiation so that it is not contributing to the photoprocess occurrence. Moreover the finding that the thickness of the TiO₂ layer deposited on the beads does not affect the results of reaction rate, conversion and selectivity, is a clear indication that the pathlength of radiation absorbed by the TiO₂ layer is less (or equal) than the thickness of the 10 layers film (3.6 μm). As a consequence only an undetermined aliquot of the total amount of TiO₂ catalyst present in the fixed bed is active for the occurrence of the photoprocess. This finding, consequence of the radiation modelling and of the reactivity experiments with different TiO₂ layers, determines an important limitation on the chemical kinetic modelling as in the present case it is not possible to confidently elucidate the influence of radiation intensity on the photoprocess kinetics.

It must be noted that the observed independency of the photoprocess rate on the number of deposited layers can not be explained by considering the diffusion of the reagent inside the film as the controlling process. For evaluating the influence of pore diffusion on the photocatalytic reaction, the Weisz-Prater (W-P) criterion (Murzin and Salmi, 2005) has been applied. The W-P number, N_{W-P} , is defined as:

$$N_{W-P} = \frac{(-r)}{V_{\text{Cat}}} \frac{\delta}{C_{\text{MBA}} D_{\text{eff}}} \quad (8)$$

in which V_{Cat} is the catalyst volume, δ the catalyst layer thickness and D_{eff} the effective diffusivity of MBA in the pores of catalyst. In the absence of specific literature data, the D_{eff} value of $10^{-10} \text{ m}^2 \text{ s}^{-1}$, found for diffusion of benzoic acid in thick layers of TiO₂ Degussa P25 (Chen et al., 2000) has been used. For the less favourable conditions the N_{W-P} value was of the order of magnitude of 10^{-3} then widely satisfying the W-P criterion.

The kinetic analysis of heterogeneous photocatalytic reactions occurring both in liquid or gas phase is generally based on the application of Langmuir-Hinshelwood (LH) rate expressions (Turchi and Ollis, 1989; Augugliaro et al., 1994; Ibrahim and de Lasa, 2004; Addamo et al., 2005b; Gora et al., 2006). The LH model has been recently questioned (Emeline et al., 2005; Ollis, 2005a; Ollis, 2005b) as it is not able to explain the experimentally observed dependence of the rate parameters on light intensity. In its simplest form the LH model assumes one fast reaction achieving adsorption equilibrium followed by a slow surface reaction step. For photocatalytic systems where adsorption-desorption is not equilibrated, the slow step approximation cannot be applied. In this case the steady state approach (Ollis, 2005b; Murzin, 2006; Serrano et al., 2007) has been applied by assuming that the surface concentrations of reacting species are in steady state. This approach leads to a kinetic expression that resembles LH kinetics but with the advantage that the model parameters explicitly depend on light

intensity. It is useful to report that the simple rate form of the LH approach, however, may have origins which take into account different photoreaction mechanisms (Demeestere et al., 2004; Minero and Vione, 2006; Krýsa et al., 2006).

The dependence of reaction rate on the MBA concentrations, shown by the experimental data of Figure 6 is of Langmuir type thus indicating that the adsorption kinetics of MBA onto the catalyst surface plays an important role in the overall rate of the process. The modelling of the photoreactivity results was performed by assuming that all the elementary reactions of MBA oxidation, both partial and total, occur on the catalyst surface involving adsorbed species, which can interact with hydroxyl groups. Owing to the fact that the reaction rate values observed in this work are not affected by external mass transfer resistance (see Figure 4) nor by diffusion inside pores as confirmed by the low value of W-P number, the rate-determining step of the process is hypothesised to be the second order reaction between HO[•] radical and the aromatic molecule adsorbed onto the catalyst surface. This simple model is commonly used to analyse the kinetics of photocatalytic reactions and it generally provides a satisfactory prediction of the progress of species concentration in liquid phase (Turchi and Ollis, 1989; Augugliaro et al., 1994; Gora et al., 2006).

The reactivity results indicate that oxygen is needed for the photoreaction to proceed. Moreover, the occurrence of two parallel pathways, i.e. partial oxidation and mineralization, suggests that the adsorption sites, responsible of these pathways, have different features. On this ground the kinetic modelling of photoreactivity results is made by assuming that three different types of site exist on the catalyst surface. The first type is able to adsorb oxygen so that the HO[•] radical concentration depends on the fractional sites coverage by O₂ (as the adsorbed oxygen acts as an electron trap thus hindering the e-h recombination) the second one adsorbs the organic molecules by producing their partial oxidation and the third one adsorbs the organic molecules by eventually producing their mineralization.

Under these hypotheses the disappearance rate of MBA per unit surface area ($-r_{\text{MBA}}$) for second order reactions in parallel (partial oxidation and mineralization) has been modelled in terms of Langmuir-Hinshelwood kinetics as:

$$(-r_{\text{MBA}}) = \frac{(-r)}{S} = k_{\text{PO}}\theta_{\text{Ox}}\theta_{\text{PO}} + k_{\text{MIN}}\theta_{\text{Ox}}\theta_{\text{MIN}} \quad (9)$$

in which S is the surface area of the irradiated catalyst, k_{PO} and k_{MIN} are the second order rate constants for partial oxidation and mineralization, respectively, θ_{Ox} the fractional site coverage of oxygen, and θ_{PO} and θ_{MIN} the fractional coverages of MBA on sites determining its partial oxidation to PAA or its mineralization to CO₂, respectively. The specific rates of PAA production, r_{PAA} , and of MBA mineralization, r_{MIN} , are obviously:

$$r_{\text{PAA}} = k_{\text{PO}}\theta_{\text{Ox}}\theta_{\text{PO}} \quad (10)$$

$$r_{\text{MIN}} = k_{\text{MIN}}\theta_{\text{Ox}}\theta_{\text{MIN}} \quad (11)$$

The photoreactivity run carried out with PAA showed that it may participate both to partial oxidation reaction producing 4-methoxybenzoic acid and to mineralization reaction producing CO₂. This finding suggests that in the course of MBA oxidation, the produced PAA may compete with MBA for adsorption both on the partial oxidising and mineralising sites. On this ground the fractional site coverages of eqn. 9 may be written in terms of the Langmuir relationship as:

$$\theta_{\text{Ox}} = \frac{K_{\text{Ox}}C_{\text{Ox}}}{1 + K_{\text{Ox}}C_{\text{Ox}}} \quad (12)$$

$$\theta_{\text{PO}} = \frac{K_{\text{PO}}C_{\text{MBA}}}{1 + K_{\text{PO}}(C_{\text{MBA}} + C_{\text{PAA}})} \quad (13)$$

$$\theta_{\text{MIN}} = \frac{K_{\text{MIN}} C_{\text{MBA}}}{1 + K_{\text{MIN}} (C_{\text{MBA}} + C_{\text{PAA}})} \quad (14)$$

where C_{Ox} , C_{MBA} and C_{PAA} are the oxygen, MBA and PAA concentrations in the aqueous phase, whereas K_{Ox} , is the equilibrium adsorption constant of oxygen, and K_{PO} and K_{MIN} those of MBA and PAA on partial oxidising and mineralising sites, respectively. Equations 13 and 14 are written under the hypothesis that the equilibrium adsorption constants of MBA and PAA on those sites are similar (Turchi and Ollis, 1989; Augugliaro et al. 1994, Palmisano et al., 2007b).

By considering that for all the runs MBA conversion was always lower than 8%, the assumptions are here made that the photoreactor behaves as a differential one and that the oxygen concentration in the liquid phase does not substantially changes from the inlet to the outlet of photoreactor, i.e. the oxygen fractional site coverage remains constant for all the runs. On this ground by substituting eqns. 13 and 14 in eqns. 10 and 11 and by introducing the concentration values averaged between the inlet and outlet of the photoreactor, the following relationships are obtained after some arrangements:

$$\frac{S k'_{\text{PO}}}{Q C_{\text{PAA},\text{O}}} = \frac{2}{K_{\text{PO}}} \frac{1}{C_{\text{MBA},\text{I}} + C_{\text{MBA},\text{O}}} + \frac{C_{\text{PAA},\text{O}}}{C_{\text{MBA},\text{I}} + C_{\text{MBA},\text{O}}} + 1 \quad (15)$$

$$\frac{S k'_{\text{MIN}}}{Q (C_{\text{MBA},\text{I}} - C_{\text{MBA},\text{O}} - C_{\text{PAA},\text{O}})} = \frac{2}{K_{\text{MIN}}} \frac{1}{C_{\text{MBA},\text{I}} + C_{\text{MBA},\text{O}}} + \frac{C_{\text{PAA},\text{O}}}{C_{\text{MBA},\text{I}} + C_{\text{MBA},\text{O}}} + 1 \quad (16)$$

where $C_{\text{PAA},\text{O}}$ is the outlet PAA concentration, $k'_{\text{PO}} = k_{\text{PO}} \theta_{\text{Ox}}$ and $k'_{\text{MIN}} = k_{\text{MIN}} \theta_{\text{Ox}}$. By substituting in eqns. 15 and 16 the experimental values of $C_{\text{MBA},\text{I}}$, $C_{\text{MBA},\text{O}}$ and $C_{\text{PAA},\text{O}}$ obtained from each run and by applying a least-squares best fitting procedure, the values of $S k'_{\text{PO}}$, $S k'_{\text{MIN}}$, K_{PO} and K_{MIN} have been obtained ($R^2 > 0.96$). This non linear fit was carried out by using the curve-fitting function available in Mathematica version 4 (Wolfram Media). For both the catalysts the same values were obtained: these values together with the corresponding 90 % confidence intervals are $S k'_{\text{PO}} = 2.043 \pm 0.134 \cdot 10^{-8} \text{ mol} \cdot \text{s}^{-1}$, $S k'_{\text{MIN}} = 2.90 \pm 0.182 \cdot 10^{-8} \text{ mol} \cdot \text{s}^{-1}$ and $K_{\text{PO}} = 900 \pm 56 \text{ M}^{-1}$, $K_{\text{MIN}} = 5000 \pm 450 \text{ M}^{-1}$.

It may be noted that the product between the kinetic constants and the irradiated surface area of the catalyst, S , are here reported. The S parameter is very difficult to be confidently determined only with the information obtained in this work. Due to the uncertainties related to S , it has been decided to leave this parameter as an unknown.

6. CONCLUSIONS

The photocatalytic oxidation of 4-methoxybenzyl alcohol in aqueous solution by using a fixed bed continuous photoreactor containing Pyrex beads covered by a thin film of home prepared TiO_2 photocatalyst occurs through two parallel routes: the first is a partial oxidation producing p-anisaldehyde and the second one is a mineralization. The modelling of radiation field inside the photoreactor allows one to determine that the radiation intensity profile sharply decreases inside the bed so that an important aliquot of the bed is not active for the photoreaction occurrence; moreover it is found that the penetration depth of radiation in the TiO_2 film is less (or equal) than the film thickness. The finding that an aliquot of the TiO_2 catalyst present in the fixed bed is not working determines that the reactivity results can not be used jointly with the radiation modelling ones for determining the dependence of reaction kinetics on light intensity. It is important, however, to outline that the kinetic modelling and its main result, i.e. that two types of active site must be present on the TiO_2 surface, hold even if a part of photocatalyst is not active. The true values of the Langmuir-Hinshelwood model parameters will be known once the amount of active catalyst is surely determined. Work is in progress on this specific point.

REFERENCES

- Addamo M., Augugliaro V., Di Paola A., García-López E., Loddo V., Marci G., Palmisano L., "Preparation and photoactivity of nanostructured TiO₂ particles obtained by hydrolysis of TiCl₄", *Colloids and Surfaces A: Physicochem Eng Aspects*, Vol. 265, No. 5, 23–31 (2005) a.
- Addamo M., Augugliaro V., Coluccia S., Faga M.G., García-López E., Loddo V., Marci G., Martra G., Palmisano L., "Photocatalytic oxidation of acetonitrile in gas-solid and liquid-solid regimes", *J Catal.*, Vol. 235, No. 22, 209-220 (2005) b.
- Alexiadis A., "2-D radiation field in photocatalytic channels of square, rectangular, equilateral triangular and isosceles triangular sections", *Chem Eng Sci.*, Vol. 61, No. 18, 516-525 (2006).
- Almquist C.B., Biswas P., "The photo-oxidation of cyclohexane on titanium dioxide: an investigation of competitive adsorption and its effects on product formation and selectivity", *Appl Catal A: Gen.*, Vol. 214, No. 13, 259-271 (2001).
- Augugliaro V., Cavallero L., Marci G., Palmisano L., Pramauro E., "Influence of operational variable on the photodegradation kinetics of monuron in aqueous titanium dioxide dispersions", in "New Developments in Selective Oxidation II" V. Cortés Corberan, S. Vic Bellon Eds., Elsevier Science Publishers B. V., The Netherlands, Amsterdam, 713-720 (1994).
- Bird R.B., Stewart W.E., Lightfoot E.N., "Transport phenomena", Wiley, New York: (1960).
- Caronna T., Gambarotti C., Palmisano L., Punta C., Recupero F., "Sunlight-induced reactions of some heterocyclic bases with ethers in the presence of TiO₂. A green route for the synthesis of heterocyclic aldehydes", *J Photochem Photobiol A.*, Vol. 171, No. 3, 237-242 (2005).
- Cassano A.E., Martín C.A., Brandi R.J., Alfano O.M., "Photoreactor analysis and design: fundamentals and applications", *Ind. Eng. Chem. Res.*, Vol. 34, No. 7, 2155-2201 (1995).
- Cermenati L., Dondi D., Fagnoni M., Albini A., "Titanium dioxide photocatalysis of adamantane", *Tetrahedron*, Vol. 59, No. 34, 6409-6414 (2003).
- Changrani R., Raupp G.B., "Monte Carlo simulation of the radiation field in a reticulated foam photocatalytic reactor", *AIChE J.*, Vol. 45, No. 5, 1085-1094 (1999).
- Changrani R., Raupp G.B., "Two-dimensional heterogeneous model for a reticulated-foam photocatalytic reactor", *AIChE J.*, Vol. 46, No. 4, 829-842 (2000).
- Chen D., Li F., Ray A.K., "Effect of mass transfer and catalyst layer thickness on photocatalytic reaction" *AIChE J.*, Vol. 46, No. 5, 1034-1045 (2000).
- Coronado J.M., Soria J., Conesa J.C., Bellod R., Adán C., Yamaoka H., Loddo V., Augugliaro V., "Photocatalytic inactivation of Legionella Pneumophila and aerobic bacteria consortium in water over TiO₂/SiO₂ fibres in a continuous reactor", *Topics in Catalysis*, Vol. 35, No. 3-4, 279-286 (2005).
- de Lasa H., Serrano B., Salices M., "Photocatalytic reaction engineering", Springer Dordrecht, (2005).
- Demeestere K., De Visscher A., Dewulf J., Van Leeuwen M., Van Langenhove H., "A new kinetic model for titanium dioxide mediated heterogeneous photocatalytic degradation of trichloroethylene in gas-phase", *Appl. Catal. B: Environ.*, Vol. 54, No. 4, 261-274 (2004).
- Emeline A.V., Ryabchuk V.K., Serpone N., "Dogmas and misconceptions in heterogeneous photocatalysis. Some enlightened reflections" *J. Phys. Chem. B.*, Vol. 109, No. 39, 18515-18521 (2005).

Farhadi S., Afshari M., Maleki M., Babazadeh Z., "Photocatalytic oxidation of primary and secondary benzylic alcohols to carbonyl compounds catalyzed by $\text{H}_3\text{PW}_{12}\text{O}_{40}/\text{SiO}_2$ under an O_2 atmosphere", *Tetrahedron Lett.*, Vol. 46, No. 49, 8483-8486 (2005).

Fujishima A., Hashimoto K., Watanabe T., "TiO₂ photocatalysis. Fundamentals and applications", BKC, Inc., Tokyo (1999).

Fujishima A., Rao T.N., Tryk D.A., "Titanium dioxide photocatalysis", *J. Photochem. Photobiol. C: Photochem. Rev.*, Vol. 1, No. 1, 1-21 (2000).

Gora A., Toepfer B., Puddu V., Li Puma G., "Photocatalytic oxidation of herbicides in single-component and multicomponent systems: reaction kinetics analysis", *Appl Catal B: Environ.*, Vol. 65, No. 1-2, 1-10 (2006).

Hoffmann M.R., Martin S.T., Choi W., Bahnemann D.W., "Environmental applications of semiconductor photocatalysis". *Chem. Rev.*, Vol. 95, No. 1, 69-96 (1995).

Ibrahim H., de Lasa H., "Kinetic modelling of the photocatalytic degradation of air-borne pollutants" *AIChE J.*, Vol. 50, No. 5, 1017-1027 (2004).

Imoberdorf G.E., Alfano O.M., Cassano A.E., Irazoqui H.A., "Monte Carlo model of the interaction between UV-radiation and TiO₂-coated spheres" *AIChE J.*, submitted, (2007).

Krýsa J., Waldner G., Měšťánková H., Jirkovský J., Grabner G., "Photocatalytic degradation of model organic pollutants on an immobilized particulate TiO₂ layer. Roles of adsorption processes and mechanistic complexity" *Appl. Catal. B: Environ.*, Vol. 64, No. 3-4, 290-301 (2006).

Li C., Chen L., "Organic chemistry in water", *Chem. Soc. Rev.*, Vol. 35, No. 1, 68-82 (2006).

Minero C., Vione D., "A quantitative evaluation of the photocatalytic performance of TiO₂ slurries", *Appl. Catal. B: Environ.*, Vol. 67, No. 3-4, 257-269 (2006).

Mohamed O.S., El-Aal A., Gaber M., Abdel-Wahab A.A., "Photocatalytic oxidation of selected aryl alcohols in acetonitrile", *J. Photochem. Photobiol. A.*, Vol. 148, No. 1, 205-210 (2002).

Murzin D.Y., "Heterogeneous photocatalytic kinetics: beyond the adsorption/desorption equilibrium concept", *React. Kinet. Catal. Lett.*, Vol. 89, No. 2, 277-284 (2006).

Murzin D.Y., Salmi T., "Catalytic kinetics", Amsterdam: Elsevier, (2005).

Narayan S., Muldoon J., Finn M.G., Fokin V.V., Kolb H.C., Barry Sharpless K., "On water: unique reactivity of organic compounds in aqueous suspension" *Angew. Chem. Int. Ed.*, Vol. 44, No. 21, 3275-3279 (2005).

Ohtani B., Pal B., Ikeda S., "Photocatalytic organic syntheses: selective cyclization of amino acids in aqueous suspensions", *Catal. Surv. Asia.*, Vol. 7, No. 2-3, 165-176 (2003).

Ollis D.F., Al-Ekabi H., "Photocatalytic purification and treatment of water and air", New York: Elsevier, (1993).

Ollis D.F., "Kinetics of liquid phase photocatalyzed reactions: an illuminating approach." *J. Phys. Chem. B*, Vol. 109, No. 6, 2439-2444 (2005) a.

Ollis D.F., "Kinetic disguises in heterogeneous photocatalysis", *Top. Catal.*, Vol. 35, No. 3-4, 217-223 (2005) b.

Palmisano G., Yurdakal S., Augugliaro V., Loddo V., Palmisano L., "Photocatalytic selective oxidation of 4-methoxybenzyl alcohol to aldehyde in aqueous suspension of home-prepared titanium dioxide catalyst". *Adv. Synth. Catal.*, Vol. 349, No. 6, 964-970 (2007) a.

Palmisano G., Loddo V., Yurdakal S., Augugliaro V., Palmisano L., "Photocatalytic oxidation of nitrobenzene and phenylamine: pathways and kinetics", *AIChE J.*, Vol. 53, No. 4, 961-968 (2007) b.

Pasquali M., Santarelli F., Porter J.F., Yue P.L., "Radiative transfer in photocatalytic systems", *AIChE J.*, Vol. 42, No. 2, 532-537. (1996).

Pillai U.R., Sahle-Demessie E., "Selective oxidation of alcohols in gas phase using light-activated titanium dioxide", *J. Catal.* Vol. 211, No. 2, 434-444. (2002).

Reddy B.M., Rao K.N., Reddy G.K., Bharali P., "Characterization and catalytic activity of $V_2O_5/Al_2O_3-TiO_2$ for selective oxidation of 4-methylanisole" *J. Mol. Catal. A: Chem.*, Vol. 253, No. 1-2, 44-51 2006.

Sahle-Demessie E., Gonzalez M., Wang Z., Biswas P., "Synthesizing alcohols and ketones by photoinduced catalytic partial oxidation of hydrocarbons in TiO_2 film reactors prepared by three different methods" *Indus. Eng. Chem. Res.*, Vol. 38, No. 9, 3276-3284 (1999).

Schiavello M., "Photoelectrochemistry, photocatalysis, and photoreactors. Fundamentals and developments", Dordrecht: Reidel (1985).

Schiavello M., "Heterogeneous photocatalysis", Wiley, Chichester (1997).

Serpone N., Pelizzetti E., "Photocatalysis, fundamentals and applications", Wiley, New York (1989).

Serrano B., Salaices M., Ortiz A., de Lasa H.I., "Quasi-equilibrium and non-equilibrium adsorption in heterogeneous photocatalysis", *Chem. Eng. Sci.*, in press (DOI: 10.1016/j.ces.2007.01.026), (2007).

Spadoni G., Bandini E., Santarelli F., "Scattering effects in photosensitized reactions" *Chem. Eng. Sci.*, Vol. 33, No. 4, 5174-524 (1978).

Turchi C.S., Ollis D.F., "Mixed reactant photocatalysis – intermediates and mutual rate inhibition", *J. Catal.*, Vol. 119, No. 2, 483-496 (1989).

Yang Q.Y., Ang P.L., Ray M.B., Pehkonen S.O., "Light distribution field in catalyst suspensions within an annular photoreactor" *Chem. Eng. Sci.*, Vol. 60, No. 19, 5255-5268 (2005).